

Comparison of spectral image reconstruction methods using multipoint spectral measurements

Yuri Murakami, Kunihiko Ietomi, Ayumi Tadano, Masahiro Yamaguchi, and Nagaaki Ohyama; Imaging Science & Engineering Laboratory, Tokyo Institute of Technology; Yokohama/Japan

Abstract

The accuracy of spectral image reconstruction from three-band images can be improved by utilizing multipoint spectral measurements as auxiliary information. There can be different approaches for exploiting the multipoint spectral data. In Wiener and GMD (Gaussian mixture distribution)-based estimation methods, spectral data are employed to estimate the spectral statistics of a scene. The information of spatial coordinates of each spectral data can be also used for instance, with using the spatio-spectral MAP (Maximum a posteriori) estimation. However, spatio-spectral MAP requires a relatively large amount of computation.

In this paper a novel method is presented as an alternative approach to make use of the spatial information of multipoint spectral data, called piecewise Wiener estimation. Then, we make a comparison of four methods: spectral Wiener, GMD-based, spatio-spectral MAP, and piecewise Wiener estimation algorithms. As a result, it has been found that methods that utilize the location information of each spectral measurement give higher accuracy than others.

Introduction

For high fidelity color reproduction of digital images, a spectrum-based color reproduction method has been studied [1-7]. In this method, spectral reflectance or spectral power distribution of an image is first estimated from the observed data, and then the color is calculated by using the estimated spectral information. In order to accurately estimate the spectral information as an image, a multispectral image with more than three color channels is preferable. Although there have been various types of multispectral or spectral imaging devices [8-10], any device suffers from the inherent tradeoff between spatial and spectral resolution. Therefore, in reality, it is difficult to develop a spectral imaging device with high resolutions in both spectral and spatial. Meanwhile, there have been various attempts to estimate spectral information from three measurements that are captured by conventional trichromatic sensors [11-15]. However, a set of three measurements have a limitation on accuracy, especially when the class of a target object cannot be specified.

Based on this background, a new spectral imaging approach has focused attention, in which a spectral image is estimated from two different types of measurements: a low-resolution image with high-spectral resolution and a high-resolution image with low-spectral resolution. Such measurement systems can be realized by a combination of conventional measurement devices. For instance, we can use a conventional three-band camera attached with a spectral sensor with a scanning unit, where the spectra are measured successively at multiple points in a scene by the spectral sensor. Or otherwise, a low-resolution spectral imaging device can be utilized instead of the scanning spectral sensor. For this new type of measurement system, we need a

method to reconstruct a spectral image from two different types of measurements, which is the topic dealt with in this paper. Below, we will discuss focusing on a combination of a three-band image and multipoint spectral measurements.

In order to reconstruct a spectral reflectance image from a three-band image and multipoint spectral measurements, a method based on the Maximum a posteriori (MAP) estimation has been proposed (referred to as spatio-spectral MAP: SS-MAP) [16,17]. In the SS-MAP, spectral data are spatially interpolated and it is used for compensating the spectral estimation error from a three-band image, which improves the estimation accuracy. However, since SS-MAP requires relatively large amount of computation, alternative methods are expected. Multipoint spectral data are also effectively utilized in the existing spectral estimation methods, like Wiener or GMD (Gaussian mixture distribution)-based estimation methods [18], in which the spectral data are utilized to estimate the spectral statistics of a scene, like a probability density, a correlation matrix, or principal components in a spectral space. In these methods, however, the spatial information of each spectral measurement is abandoned despite its effectiveness in SS-MAP.

In this paper, a novel method is presented as an alternative approach to make use of spatial information of multipoint spectral measurement, called piecewise Wiener estimation. Then, we make a comparison of four methods: spectral Wiener, GMD-based, SS-MAP, and piecewise Wiener estimation algorithms, to make it clear what kind of approach is effective for the spectral image reconstruction problem.

Spectral image reconstruction methods using multipoint spectral measurements

Overview

Figure 1 shows general approaches to reconstruct a spectral reflectance image from a three-band image and multipoint spectral measurements. They are classified broadly into two categories: a spectral estimation from a three-band image, and a spatial interpolation from multipoint spectral measurements. In the spectral estimation approach, a spectral correlation is estimated from multipoint spectral data and it is utilized in the spectral estimation. In the spatial interpolation approach, a spatial correlation is estimated from a three-band image and it is utilized in the spatial interpolation of spectral data. The combination of these two approaches is also possible. Focusing on the spectral estimation approach, we can find several cases: A. pixel-independent, B. pixel-value-dependent, and C. pixel-position-dependent spectral correlations.

If the Wiener estimation is applied to this problem, it is categorized into A, because a single correlation matrix is utilized in making Wiener estimation matrices. The GMD-based estimation method [18] and recently-proposed nonlinear estimation methods [11, 13-15] are all categorized into B, though each method has its original way to make multiple

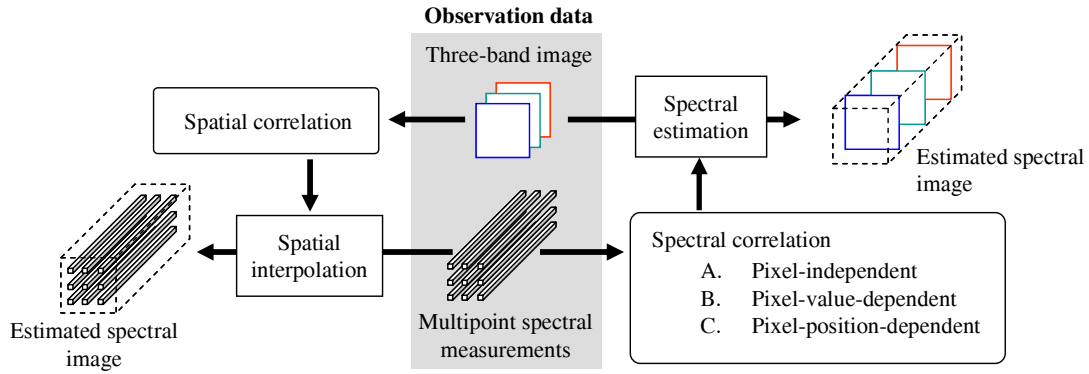


Figure 1. General approaches for the reconstruction of spectral image from three-band image and multipoint spectral measurements.

correlation matrices and the way to select a correlation matrix based on a pixel value. The SS-MAP estimation is a combination of a spatial interpolation of spectral data and a spectral Wiener estimation. On the other hand, there has been no method categorized into C, because in general it is difficult to obtain a pixel-position-dependent spectral correlation. However, it can be possible if we use the spatial information of each spectral measurement, which will be an alternate effective method.

This paper first reviews existing algorithms, and presents a method called piecewise Wiener estimation, which is categorized into C. After that, a comparison is made of four methods: Wiener, GMD-based, SS-MAP, and piecewise Wiener estimation algorithms.

Review of existing methods

Wiener estimation method

A Wiener estimation matrix is derived with using the spectral correlation matrix calculated from all the spectral measurements. Then, the spectral image is estimated from a three-band image using the Wiener estimation matrix.

GMD-based estimation method [18]

In order to apply the GMD-based estimation method, multipoint spectral measurements are clustered into several classes, which yield a GMD probability model. Then, the GMD-based estimation method gives the best spectral reflectance estimation in a minimum-mean-squared-error sense based on the obtained probability. More specifically, a spectral reflectance function is first estimated by the Wiener estimation based on the spectral correlation of each class. Then, a weighted sum of the estimated spectral reflectance functions is calculated, where the weights are decided based on the three-band image signal of a concerned pixel.

SS-MAP estimation method [17]

In the SS-MAP estimation method, multipoint spectral measurements are regarded as a low-resolution spectral image. The spectral measurements are spatially interpolated based on a spatial correlation estimated from a three-band image. On the other hand, a spectral reflectance image is estimated from the three-band image in the same manner as the Wiener estimation. Then, these two estimations of a spectral reflectance image are combined to derive the final SS-MAP estimation.

A spatial correlation used in the interpolation is an important factor in the SS-MAP estimation. The correlation between i th and j th pixel is defined by

$$r(i, j) = \mathbf{g}_i^T \mathbf{g}_j \times \rho^{d(i, j)} \quad (1)$$

where \mathbf{g}_i is a three-dimensional column vector representing a image signal of i th pixel and $d(i, j)$ is the Euclid distance between i th and j th pixels. The parameter ρ plays a role in deciding a scope of the spectral measurements that used for the interpolation. In the original manuscript, ρ is fixed at 0.97, which is selected so as to suit to the experimental condition of 100×100 spectral measurements. In this paper, ρ is variable depending on the number of the spectral measurements.

According to [17], the computational amount is in proportion to the square of the number of the spectral measurements. Therefore, it can be said that the implementation of the SS-MAP becomes difficult as increasing number of the spectral measurements.

Piecewise Wiener estimation method

This section describes the method proposed in this paper, piecewise Wiener estimation technique. In this method, a three-band image is divided into K blocks and each block is indexed by k . Wiener estimation matrix for each block, \mathbf{A}_k , is prepared, and the spectral reflectance of a pixel in a block k is estimated by the matrix \mathbf{A}_k . Each Wiener estimation matrix is derived with using the spectral correlation matrix calculated from the spectral measurements weighted by

$$w(k, j) = \rho^{D(k, j)} \quad (2)$$

where $D(k, j)$ is the Euclid distance between the center of the block k and the j th spectral measurements. The parameter ρ plays a role in deciding a scope of the spectral measurements that used for a single Wiener estimation matrix.

When different matrices are used in different blocks, signal discontinuity will arise at block boundary. In order to remove this signal discontinuity, the matrices that are assigned to the neighboring 8 blocks in addition to its own block are applied, and the estimation results are summed with a window function determined by the method in [19]. Since a window function spans a fourfold area of a block, four estimations by four different matrices are summed to derive the final estimation of a single pixel. As a result, the computation amount is approximately estimated by four times of that of Wiener estimation, because the block-dependent matrix preparation is not a dominant factor in the computation.



Figure 2. Spectral reflectance images used in the simulations: Toy, Scarf, and Flowers. Images displayed in sRGB.

Evaluation of estimation methods

Simulation conditions

Spectral reflectance images are estimated from multispectral images captured by a sixteen-band camera [6], and they are used as the true spectral reflectance images. Spatial resolution of the spectral reflectance image is 512×512 , and the number of the spectral samplings is 65 ranging from 380 to 700 nm with 5nm intervals. Figure 2 shows the three images displayed in sRGB. For convenience of demonstration, we name the three images in Fig.2 Toy, Scarf, and Flowers, respectively. Three-band images are calculated from the spectral reflectance images based on the spectral sensitivity of a typical HDTV video camera and the spectrum of daylight illuminant D65. Noise-free and noisy cases are simulated, where the noise is a Gaussian white noise with peak-signal-to-noise ratio (PSNR) is 50 dB. Spectral measurements are calculated as the average spectral reflectance functions of the true spectral reflectance image over the corresponding measurement areas. The number of the spectral measurements $M \times M$ is variable, and a measurement area is set by a $(512/M)$ -pixel square; i.e., the measurement areas are neither overlapped nor gapped. The spectral measurements are assumed to be noise free.

From a simulated three-band image and multipoint spectral measurements, a spectral reflectance image is estimated by Wiener, GMD-based, SS-MAP, and piecewise Wiener estimation methods; they are referred to as Wiener, GMD, SS-MAP, and PW in the following experimental results. The normalized root mean squared error (NRMSE) of the estimated spectral reflectance and ΔE_{ab}^* under D65 and F2 illuminants are calculated. As a reference, the estimations from 3-band and 6-band images without the information of spectral measurements are also done, where the estimation is done by a Wiener estimation matrix with the correlation matrix based on the Markov model (the correlation coefficient is set at 0.995); these are referred to as 3-band and 6-band.

The parameter ρ is defined by $\rho^{4.5(512/M)} = 0.01$ for SS-MAP and $\rho^{2(512/M)} = 0.01$ for piecewise Wiener, both of which

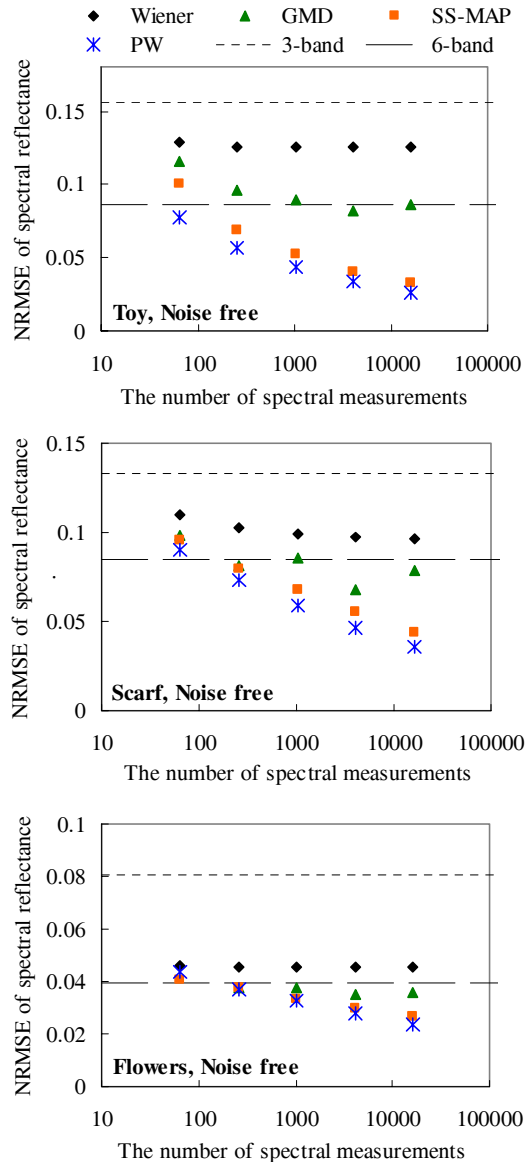


Figure 3. NRMSE of spectral reflectance of Toy (top), Scarf (middle), and Flowers (bottom) in noise-free case with varying the number of spectral measurements.

are determined empirically. The clustering for GMD is performed by a K-means clustering method, and the number of the classes is set by 5 for Toy and Scarf, and 3 for Flowers.

Results

Figure 3 shows the NRMSE of spectral reflectance of Toy, Scarf, and Flowers in noise-free case. The x axis is the number of the spectral measurements in a log-scale. The NRMSEs of 3-band and 6-band are designated by horizontal dotted and dashed lines. We can see that the four methods with spectral measurements, Wiener, GMD, SS-MAP, and PW, reduce the error from the 3-band result. Although the error is decreasing as increasing the number of the spectral measurements except for Wiener, we can see that SS-MAP and PW realize lower NRMSE than GMD, and that PW is slightly better than SS-MAP. With the spectral measurements more than several hundred, SS-MAP and PW give smaller NRMSE than 6-band.

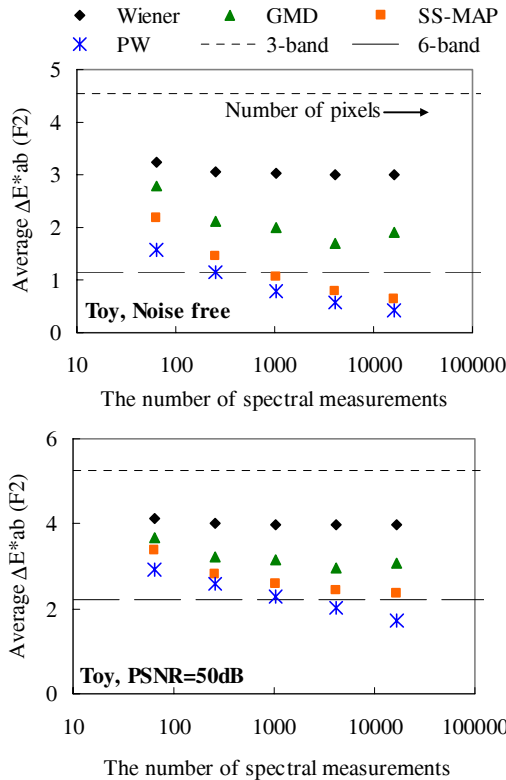


Figure 4. Average ΔE_{ab}^* of Toy in noise-free case (top) and in 50dB-noise case (bottom) with varying the number of spectral measurements.

Figure 4 shows the average ΔE_{ab}^* of Toy under F2 illuminant in noise-free and noisy cases. The average error shows approximately the same tendency as the NRMSE in Fig.3. In the noisy case, with more than several-thousand spectral measurements, SS-MAP does not reduce the average error even as increasing the number of the spectral measurements, while PW shows the improvement in this range.

Figure 5 shows the maximum ΔE_{ab}^* of Toy under F2 illuminant in noise-free and noisy cases. The order among four methods is almost same as that of the average results, though PW shows its slight instability. This instability is caused by the fact that the variety of the spectral measurements becomes too small to construct a correlation matrix when the total number of the spectral measurements becomes large, which may be improved by adjustment of the parameter ρ .

In addition, in the noisy case, we can see that it is difficult to reduce the maximum error even with a large number of multipoint spectral measurements. In general, in order to reduce the average error for a given data set, the relation between a three-band image and the estimated spectral reflectance becomes increasingly more complex. Complex estimations tend to be instable especially for noisy data, which causes the large maximum errors. We have examined the pixels with the error around the maximum error in the reconstructed images, and found that they are single pixels and they do not have visually much effect on the reproduced images. The results on color differences for Scarf and Flowers show the similar tendency to the Toy results. As a result, from the viewpoint of color reproduction error, SS-MAP and PW also shows superiority

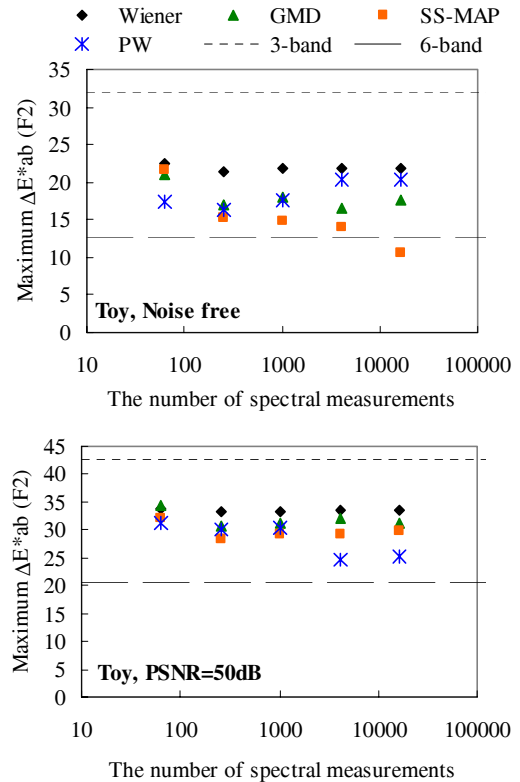


Figure 5. Maximum ΔE_{ab}^* of Toy in noise-free case (top) and in 50dB-noise case (bottom) with varying the number of spectral measurements.

than Wiener and GMD, and the difference between SS-MAP and PW is quite small, which can be seen with a large number of spectral measurements.

Figure 6 presents the visualized ΔE_{ab}^* images of Toy (left column) and Scarf (right column) under F2 illumination in noise-free case. The number of the spectral measurements is 16×16 for Toy and 64×64 for Scarf, and an 8-bit pixel value corresponds to $\Delta E_{ab}^* \times 10$ for Toy and $\Delta E_{ab}^* \times 20$ for Scarf. In the Toy results, we can see that a large error occurs, especially in the upper-left object (red color) and its right-hand neighbor (green color) by 3-band and Wiener. These errors are reduced by GMD, SS-MAP and PW. Although the average error of 6-band is smaller than that of SS-MAP and PW, we can found the areas in which SS-MAP and PW realize a smaller error than 6-band; for instance, a plate with characters placed below the image center.

In the results of Scarf, we can see a similar tendency with the Toy results. However, examining the error images in detail, it is found that the error tends to remain in high-spatial-frequency areas in the case of the method using multipoint spectral measurements. In order to see it clearly, Fig.7 shows a close-up view of the error image of Scarf, showing a region including both high- and low-spatial-frequency areas. Compared to the 3-band result, we can apparently see that the methods using spectral data more reduce the error in low-frequency area than in high-frequency area. In addition, SS-MAP shows this tendency stronger than GMD and PW. This is because the SS-MAP is partly based on a spatial interpolation.

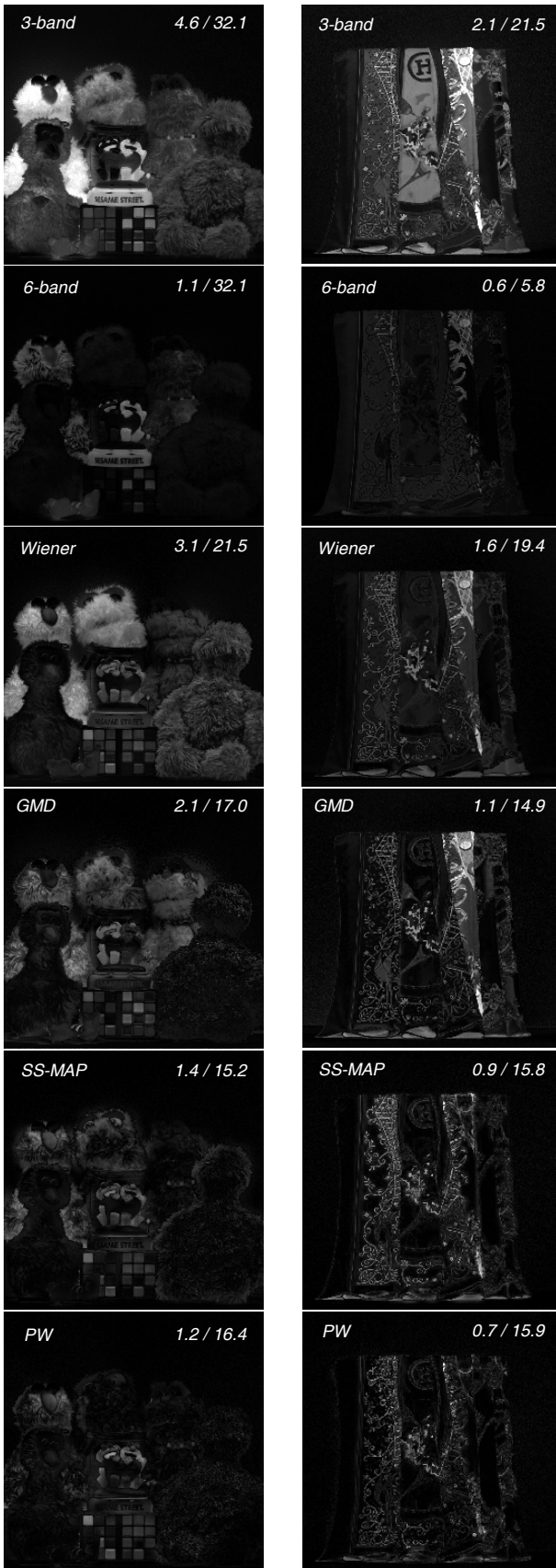


Figure 6. Visualized ΔE_{ab}^* images of Toy (left) and Scarf (right) under F2 illumination in noise-free case. The number of spectral measurements is 16×16 for Toy and 64×64 for Scarf, and an 8-bit pixel value corresponds to $\Delta E_{ab}^* \times 10$ for Toy and $\Delta E_{ab}^* \times 20$ for Scarf. The upper-right figures indicate average ΔE_{ab}^* / maximum ΔE_{ab}^* .

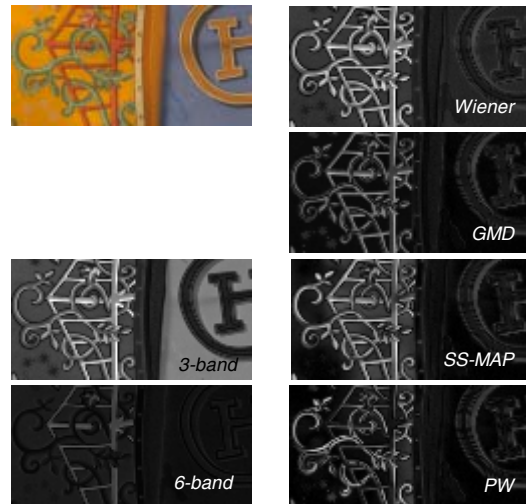


Figure 7. Close-up view of the error image of Scarf in Fig.6. The top-left color image is the original of the corresponding area.

Based on the results of the average ΔE_{ab}^* , the feature of the error distribution, and the computational cost, it can be concluded that PW is the most effective method among the four.

Conclusions

The estimation accuracy of the four methods, Wiener, GMD-based, SS-MAP, piecewise Wiener, are compared, and it is found that SS-MAP and piecewise Wiener estimation give higher accuracy than others. The SS-MAP and the piecewise Wiener estimations are the methods that make use of the spatial information of the spectral measurements, while other two use the spectral measurements to estimate a statistical data only. This result indicates the importance of utilizing the spatial information of spectral measurements in reconstructing spectral image. The importance increases especially when the number of the spectral measurements is large. In addition, SS-MAP shows a relatively strong nonuniformity in the error distribution; the error tends to remain in high-spatial-frequency areas. This is considered as an inherent feature of a method based on a spatial interpolation. Then, it should be said that an interpolation-based method may have its unsuitable scenes or applications. Based on the above experimental results and the consideration on the computational cost, it can be concluded that the piecewise Wiener estimation is the most promising method at the current moment.

This research is supported by the National Institute of Information and Communications Technology (NICT).

References

- [1] P. D. Berns and R. S. Berns, Analysis of multispectral image capture, Proc. CIC, pg. 19 (1996).
- [2] M. Hauta-Kasari, K. Miyazawa, S. Toyooka, and J. Parkkinen, "Spectral vision system for measuring color images," J. Opt. Soc. A, 16, 2352 (1999).
- [3] B. Hill, Color capture, color management and the problem of metamerism, Proc. SPIE 3963, pg. 3. (2000).
- [4] H. Haneishi, T. Hasegawa, A. Hosoi, Y. Yokoyama, N. Tsumura and Y. Miyake, "System design for accurately estimating spectral reflectance of art paintings," Appl. Opt., 39, 6621 (2000).
- [5] J. Y. Hardeberg, F. Schmitt, and H. Brettel, "Multispectral color image capture using a liquid crystal tunable filter," Opt. Eng., 41, 2532 (2002).

- [6] M. Yamaguchi, T. Teraji, K. Ohsawa, T. Uchiyama, H. Motomura, Y. Murakami, N. Ohyama, Color image reproduction based on the multispectral and multiprimary imaging: Experimental evaluation, Proc. SPIE 4663, pg. 15. (2002).
- [7] M. Yamaguchi, H. Hideaki, H. Fukuda, J. Koshimoto, H. Kanazawa, M. Tsuchida, R. Iwama, and N. Ohyama, High-fidelity video and still-image communication based on spectral information: Natural Vision system and its applications, Proc. SPIE 6062, pg. G12. (2006).
- [8] H. Sugiura, T. Kuno, N. Watanabe, N. Matoba, J. Hayashi and Y. Miyake, Development of highly accurate multispectral cameras, Proc. International Symposium on Multispectral Imaging and Color Reproduction for Digital Archives, pg. 21 (1999).
- [9] H. Fukuda, T. Uchiyama, H. Haneishi, M. Yamaguchi and N. Ohyama, Development of 16-band multispectral image archiving system, Proc. SPIE 5667, pg. 136 (2002).
- [10] K. Ohsawa, T. Ajito, H. Fukuda, Y. Komiya, H. Haneishi, M. Yamaguchi and N. Ohyama, "Six-band HDTV camera system for spectrum-based color reproduction," J. Imag. Sci. and Tech. 48, 85-92 (2004).
- [11] J. M. DiCarlo and B. A. Wandell, "Spectral estimation theory: beyond linear but before Bayesian," J. Opt. Soc. A, 20, 1261 (2003).
- [12] P. Morovic and G. D. Finlayson, "Metamer -set-based approach to estimating surface reflectance from camera RGB," J. Opt. Soc. Am. A, 23, 1814 (2006).
- [13] F. A. Jose, F. Echavarii, and P. Renet, "Use of three tristimulus values from surface reflectance spectra to calculate the principal components for reconstructing these spectra by using only three eigenvectors," J. Opt. Soc. Am. A, 23, 2020 (2006).
- [14] H. Shen, P. Cai, S. Shao, and J. H. Xin, "Reflectance reconstruction for multispectral imaging by adaptive Wiener estimation," Optics Express, 15, 15545 (2007).
- [15] X. Zhang and H. Xu, "Reconstructing spectral reflectance by dividing spectral space and extending the principal components in principal component analysis," J. Opt. Soc. Am. A, 25, 371 (2008).
- [16] K. Ietomi, Y. Murakami, M. Yamaguchi, and N. Ohyama, MAP estimation for spectral image reconstruction using 3-band image and multipoint spectral measurements, Proc. MCS'07, pg. 53
- [17] Y. Murakami, K. Ietomi, M. Yamaguchi, and N. Ohyama, "MAP estimation of spectral reflectance from color image and multipoint spectral measurements," Appl. Opt., 46, 7068 (2007).
- [18] Y. Murakami, T. Obi, M. Yamaguchi, and N. Ohyama, "Nonlinear estimation of spectral reflectance based on gaussian mixture distribution for color image reproduction," Appl. Opt., 41, 4840 (2002).
- [19] J. S. Lim, "Image restoration by short space spectral subtraction," IEEE Trans. A coust., Speech, Signal Processing, ASSP-28, 191 (1980).

Author Biography

Yuri Murakami received her BS from Japan Women's University (1996) and her M.Eng and Ph.D from Tokyo Institute of Technology (TIT) in 19 98 and 200 5, respectively. She is presently a researcher in Imaging Science and Engineering Laboratory, TIT. From 2000 to 2004, she had been a research associate in TIT. She has been working on the color image reproduction using multispectral imaging and multispectral image compression.